Photodetachment and theoretical study of free and water-solvated nitrate anions, $NO_3^-(H_2O)_n$ ($n=0-6$)

Xue-Bin Wang, Xin Yang, and Lai-Sheng Wang[a)]
Department of Physics, Washington State University, Richland, Washington 99352 and W. R. Wiley Environmental Molecular Sciences Laboratory, Pacific Northwest National Laboratory, Richland, Washington 99352

John B. Nicholas[b)]
Genentech, Inc., South San Francisco, California 94080

(Received 1 June 2001; accepted 19 October 2001)

We investigated free and water-solvated gas phase nitrate anions, $NO_3^-(H_2O)_n$ ($n=0-6$), by photodetachment photoelectron spectroscopy and theoretical calculations. We obtained the electronic structure and electron binding energies of the free and solvated NO_3^- at three detachment photon energies, 4.661, 6.424, and 7.866 eV. The ground and two low-lying electronic excited states of the NO_3 radical ($X\ ^2A_2'$, $A\ ^2E''$, $B\ ^2E'$) were observed at the 6.424 and 7.866 eV photon energies. The photoelectron spectra of the solvated nitrate complexes are similar to that of the bare NO_3^-, except that they become broadened and diffuse due to the solvation. The spectrum of $NO_3^-(H_3O)_3$ showed a resolved vibrational progression of the N–O symmetric stretching (1000 cm^{-1}), suggesting the cluster possesses a high symmetry. NO_3^- and NO_3 were calculated at various levels of theory. Based on the good agreement between density functional theory calculations and experiment for NO_3^- and NO_3, we carried out systematic calculations for $NO_3^-(H_2O)_n$ ($n=1-6$) using primarily density function theory methods. The calculations indicate that $NO_3^-(H_2O)_n$ ($n=1-3$) are all planar, with the first three H_2O forming the first solvation shell around NO_3^-, giving rise to a highly symmetric C_{3h} $NO_3^-(H_2O)_3$. The next three waters form a second solvation shell without direct contact with NO_3^-. The C_{3h} $NO_3^-(H_2O)_3$ solvation structure was observed to be rather robust and largely preserved in the larger clusters. © *2002 American Institute of Physics.* [DOI: 10.1063/1.1427067]

I. INTRODUCTION

Gas-phase cluster spectroscopy combined with theoretical calculations has become a powerful means of obtaining atomic-level information about ion solvation and cluster structure. Unlike cations, which usually have simple solvated geometries due to the relatively large binding energies between the cation and H_2O, anion solvation is much more complicated.[1] A delicate balance between water–anion and water–water interactions determines the structure of hydrated anion clusters. For example, due to the relatively weak Cl^-–H_2O interactions, Cl^- forms a ''surface'' state in small H_2O clusters,[2] whereas strong F^-–H_2O interactions cause F^- to form an ''interior'' state.[3] Beyond the halide anions,[2–7] the most complicated solvated clusters investigated experimentally involve diatomic singly charged anions, such as I_2^- and O_2^-.[8–10] More recently, we studied the microsolvation of sulfate (SO_4^{2-}).[11] That study demonstrated a unique stepwise microsolvation pattern of the complex anion and how the water molecule stabilizes the otherwise unstable dianion molecule by molecule. Here we report an experimental and theoretical investigation of the microsolvation of another complex, yet common inorganic anion, NO_3^-.

Nitrate (NO_3^-) is a common inorganic anion in the solid state and in solution. The structure and solvation of NO_3^- in bulk solution have been extensively studied by various techniques, particularly neutron and x-ray diffractions.[1,12–14] Suggestions of the number of water molecules in the first solvation shell vary widely, from 1.7 to 17.7. This is likely due to the interference of counterions, which complicate analysis and modeling of the bulk nitrate solution. Recently, there have been a number of resonant Raman studies of bulk NO_3^- solutions.[14–16] Direct observation of NO_3^- and other anions in the atmosphere[17,18] has stimulated many studies of their detection and reactions with trace neutral molecules.[19–22] For chemical reactions involving negative ions in the atmosphere, hydration is particularly important, because water is present in the atmosphere in relatively high concentration. The hydration free energy for NO_3^- has been measured via gas-phase clustering equilibrium experiments for up to three H_2O.[23–25] There are a few *ab initio* calculations on the structure of $NO_3^-(H_2O)_n$ ($n=1-3$).[16,26,27] Knowledge of the properties of small hydrated nitrate clusters, such as their structures, free energies of hydration, and energetics, are important to understand the reactivity and chemistry of NO_3^-. Understanding the interactions of negative ions with a few waters is also the first step in providing a molecular description of the structure and energetics of these ions in aqueous solutions.

a)Electronic mail: ls.wang@pnl.gov
b)Electronic mail: jbn@gene.com

 © 2002 American Institute of Physics

Downloaded 27 Mar 2007 to 130.20.226.164. Redistribution subject to AIP license or copyright, see http://jcp.aip.org/jcp/copyright.jsp

Free NO_3^- is well known to have a D_{3h} structure with a closed-shell configuration, $\ldots(e')^4(e'')^4(a_2')^2$ and a $^1A_1'$ ground state.[28,29] Removal of an electron from the three valence orbitals of NO_3^- leads to the ground ($X\ ^2A_2'$) and the first two low-lying electronic excited states ($A\ ^2E'', B\ ^2E'$) of the neutral NO_3 radical under D_{3h} symmetry. The neutral nitrate radical (NO_3) is an even more important species in atmospheric chemistry.[29] As such its chemical and physical properties have been studied extensively.[30–39] The ground and the second excited states of NO_3 have been studied by numerous optical experiments.[30–35] A vibrationally resolved photoelectron spectroscopy (PES) study has accessed the optically "dark" first excited state of NO_3.[39] However, there have been no PES studies on the $B\ ^2E'$ state, which requires high photon energies.

In the current work, we present a combined PES and theoretical study of the free and solvated nitrate, $NO_3^-(H_2O)_n$ ($n=0-6$). A simple vibrational progression was observed for the $B\ ^2E'$ state with a 850 cm^{-1} spacing. We show that higher photon energies are necessary to study the $NO_3^-(H_2O)_n$ species using PES due to their high electron binding energies. We observed that the electron binding energies of $NO_3^-(H_2O)_n$ increase with the number of waters. The first three waters each increase the binding energy by ~0.5 eV, whereas the fourth and fifth water only increase the binding energy each by ~0.2 eV. For $NO_3^-(H_2O)_3$, we also obtained a vibrationally resolved spectrum, with a vibrational progression along the N–O symmetric stretching mode, suggesting a high symmetry structure for this solvated cluster. Extensive calculations were performed for NO_3^- at various levels of theory to assess the optimal theoretical models for the larger solvated systems. Good agreement was obtained between the experimental data and calculated electron binding energies for the free and solvated NO_3^- using density functional theory (DFT) methods. Our theoretical results show that the first three waters bind to NO_3^- in a planar geometry each forming a strong and weaker H bonds with NO_3^- oxygens. A high symmetry structure was obtained for $NO_3^-(H_2O)_3$ (C_{3h}), consistent with our experimental observation of the vibrationally resolved PES spectrum for this species. We show that the first three waters form a solvation shell around NO_3^-, whereas additional waters begin to fill the second solvation shell without direct interactions with NO_3^-.

II. EXPERIMENTAL METHOD

The experiments were performed with a magnetic-bottle time-of-flight (TOF) PES apparatus coupled to an ESI source, which has been described in detail previously.[40] Briefly, a 10^{-3} M solution of $NaNO_3$ in a water/methanol (30/70 ratio) mixed solvent was sprayed through a 0.01-mm-diam syringe needle biased at −2.2 kV. The resulting charged droplets were fed into a desolvation capillary heated to ~50 °C. Anions formed in the desolvation capillary were guided by a rf-only quadruple device into an ion trap. Ions were accumulated for 0.1 s in the ion trap before being pulsed into the extraction zone of a TOF mass spectrometer. The major anion signals were the $NO_3^-(H_2O)_n$ series. Each anion of interest was mass selected and decelerated before detachment by either an excimer laser (193 and 157 nm) or a YAG laser (266 nm) in the current study. Photoelectron TOF spectra were collected and converted to kinetic energy spectra, calibrated by the known spectra of I^- and O^-. The electron energy resolution was $\Delta E/E \sim 2\%$, i.e., 20 meV for 1 eV electrons at full deceleration of the parent anion beams.

III. THEORETICAL METHODS

$NO_3^-(H_2O)_n$ ($n=0-6$) were all initially optimized with DFT, employing the B3LYP[41] hybrid exchange–correlation functional and the 6-311+G* basis set. More accurate B3LYP geometries and detachment energies were obtained using the correlation-consistent polarized basis sets,[42] with the corresponding diffuse functions,[43] referred to as aug-cc-pVXZ, where *X* indicates the basis set zeta. For NO_3^- and NO_3, calculations were also done using these basis sets without the diffuse functions (cc-pVXZ). For some cases calculations were also done using second-order Møller–Plesset perturbation theory (MP2).[44] In addition, for NO_3^- and NO_3 we obtained energies at the coupled cluster single, double (triple) CCSD(T)/aug-cc-pVDZ and CCSD(T)/aug-cc-pVTZ levels,[45] as well as at the MP3 and MP4 levels of theory. Frequencies of all species were obtained analytically to verify that all the obtained structures are stable points on the potential energy surfaces. The frequency data (zero-point energies and other thermal contributions) were also used to estimate the solvation enthalpies and free energies of NO_3^-. We computed the vertical detachment energy (VDE) as the difference in total energy between the optimized anions and the neutral complexes at the anion geometry. We obtained the adiabatic detachment energy (ADE) as the difference in energy between the anion and the neutral both at their optimized geometries. We used GAUSSIAN 98 for all the theoretical calculations.[46] Error estimates for the theoretical ADE and VDE values are difficult to determine and have not been attempted. In many past studies we have generally been able to obtain agreement with experimental values to within ~0.1 eV.

IV. EXPERIMENTAL RESULTS

A. Photoelectron spectra of NO_3^-

The PES spectra of NO_3^- at two photon energies are shown in Fig. 1. The 193 nm spectrum shows three distinct detachment bands between 3.8 and 6.1 eV, labeled *X*, *A*, and *B*. These correspond to the ground ($X\ ^2A_2'$) and the two lowest excited states ($A\ ^2E'', B\ ^2E'$) of NO_3. The *X* and *A* bands agree well with the better resolved spectrum reported previously by Neumark *et al.*[39] Our 193 nm spectrum revealed a well-resolved vibrational progression for the *B* state with a 850 cm^{-1} vibrational spacing. We also measured the spectrum of NO_3^- at 157 nm [Fig. 2(a)], but did not observe any new transitions. The electron affinity of NO_3, determined from the 0–0 transition of the *X* band from the 266 nm spectrum, is 3.92±0.03 eV, in good agreement with the previous measurement (3.937±0.014 eV).[39] We obtained a term value for the $B\ ^2E'$ state at 1.86 eV, in excellent agreement

Downloaded 27 Mar 2007 to 130.20.226.164. Redistribution subject to AIP license or copyright, see http://jcp.aip.org/jcp/copyright.jsp

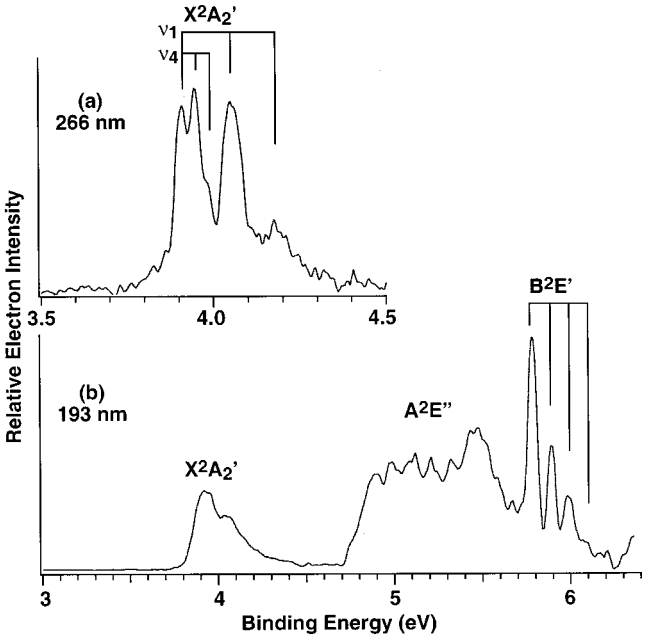

FIG. 1. Photoelectron spectra of NO_3^- at (a) 266 nm (4.661 eV) and (b) 193 nm (6.424 eV). The vertical lines indicate vibrational structures.

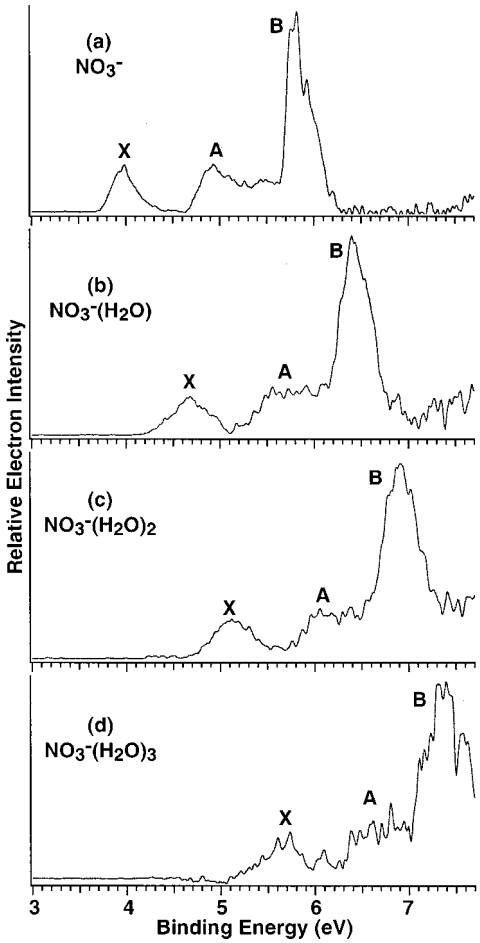

FIG. 2. Photoelectron spectra of $NO_3^-(H_2O)_n$ at 157 nm (7.866 eV). (a) NO_3^-, (b) $NO_3^-(H_2O)$, (c) $NO_3^-(H_2O)_2$, and (d) $NO_3^-(H_2O)_3$.

with previous absorption measurements (1.87 eV).[30,47] The spectroscopic data for NO_3 are given in Table I and compared with previous measurements.

B. Solvated clusters, $NO_3^-(H_2O)_n$ ($n=1-5$)

Figure 2 shows the 157 nm spectra of $NO_3^-(H_2O)_n$ ($n=1-3$) compared with that of NO_3^-. The overall spectral patterns of the solvated species are very similar to that of NO_3^-, with the expected shift to higher electron binding energies with increasing solvent numbers. These results indicate that the electronic features of NO_3^- are maintained in the solvated species. Due to the low ion intensity and low photon flux at 157 nm, larger solvated species were not able to be investigated at this wavelength. The spectrum of $NO_3^-(H_2O)_3$ already had very low electron count rates and poor statistics [Fig. 2(d)]. At 193 nm, we were able to obtain data for the solvated species up to five waters (Fig. 3). Due to the lower photon energy at 193 nm, we could only observe the *X* and *A* bands for $n=1$ and 2, the *X* band for $n=3$ and 4, and a partial *X* band for $n=5$. Again due to the low ion intensity, as well as the increased electron binding energies, we were not able to obtain data beyond $n=5$ at 193 nm. The spectra of the solvated species were all broadened and diffuse probably due to the presence of low frequency vibrational modes and the lowering of symmetry. Surprisingly, a vibrational progression was partially resolved in the spectrum of $NO_3^-(H_2O)_3$ with an average vibrational spacing of $\sim$1000 cm^{-1}, approximately corresponding to the symmetric N–O stretching. This observation suggests that $NO_3^-(H_2O)_3$ may possess a higher symmetry than the other solvated species.

The ADEs are measured from the 0–0 transition of the *X* band. Due to the broad nature of the spectra of the solvated species, only estimates of the ADEs could be obtained, as given in Table II and indicated by the arrows in Fig. 3. The VDEs were obtained from the band maxima of the ground state transition and are also given in Table II. The ADEs and VDEs were observed to increase steadily, but not linearly, with the number of waters. The incremental increase of ADE is 0.5 eV for the first three waters, and drops to $\sim$0.2 eV for $n=4$ and 5. These results suggest that the first three waters interact strongly with NO_3^- whereas the fourth and fifth waters interact more weakly. This observation and the resolved vibrational structure in $NO_3^-(H_2O)_3$ will be born out in our theoretical results presented next.

V. THEORETICAL RESULTS

A. NO_3^-

We did the most extensive calculations for NO_3^- and NO_3, as these small species allowed us to assess the accuracy of the various theoretical methods. There is evidence in the literature that the geometry of NO_3 is sensitive to the theoretical methods used to describe its electronic structure,[38] with both D_{3h} and C_{2v} symmetries reported. This is due to symmetry breaking of the Hartree–Fock wave function. Multireference configuration interaction appears to be the only traditional method by which an accurate description of the electronic structure of NO_3 can be obtained. Whereas

Downloaded 27 Mar 2007 to 130.20.226.164. Redistribution subject to AIP license or copyright, see http://jcp.aip.org/jcp/copyright.jsp

TABLE I. Observed adiabatic electron detachment energies (ADEs), term values, and vibrational frequencies for NO_3.

	ADE (eV)		Term value (eV)		Frequencies (cm^{-1})	
	Current	Previous	Current	Previous	Current	Previous
$X\ ^2A_2'$	3.92 (0.03)	3.937 (0.014)[a]	0	0	1050 (50)(ν_1)	1050[b]
					320(50)(ν_4)	360[b]
$A\ ^2E''$	4.78 (0.03)		0.86 (0.03)	0.868 (0.014)[a]	850(50)(ν_1)	804[a]
$B\ ^2E'$	5.78 (0.03)		1.86 (0.03)	1.87[b]	850 (50)[c]	850[b]

[a]Reference 39.
[b]Reference 47.
[c]In-plane bending mode (see the text).

DFT has been shown to suffer much less from symmetry breaking in the case of NO_3 and also appears to give reasonable predictions of the geometries and energies of the other species under study here, it was used for almost all of the calculations. Some limited results are presented using MP2 and CCSD(T), as detailed in the following.

Optimizations of NO_3^- were done using both B3LYP and MP2 methods, with both the cc-pVXZ and aug-cc-pVXZ (X=D, T, Q, and 5) basis sets. NO_3^- has D_{3h} symmetry with a $^1A_1'$ electronic state. At the B3LYP level, the N–O partial double bond ranges in length from 1.2614 to 1.2565 Å as the basis set is increased in size from cc-pVDZ to cc-pV5Z. Using the corresponding aug-cc-pVXZ basis sets, the bond length ranges from 1.2625 to 1.2565 Å. The charge on oxygen ranges from -0.440 to -0.437 $|e|$ with the cc-pVXZ basis sets, and from -0.687 to -0.585 $|e|$ with the aug-cc-pVXZ basis sets. The B3LYP/cc-pVDZ frequency calculations give values of 713.3 (e'), 849.4 (a_2''), 1072.7 (a_1'), and 1459.3 (e') cm^{-1}. At the B3LYP/aug-cc-pVDZ level, the frequencies are 697.6 (e'), 833.2 (a_2''), 1071.3 (a_1'), and 1390.0 (e') cm^{-1}.

B3LYP/cc-pVXZ (X=D, T, and Q) optimizations of NO_3 starting from a C_{2v} structure all resulted in D_{3h} geometries, thus the D_{3h} structure ($^2A_2'$) appears to be the ground state with this exchange–correlation functional. At the B3LYP level, the N–O partial double bond ranges in length from 1.2354 to 1.2303 Å as the basis set is increased in size from cc-pVDZ to cc-pV5Z. Using the corresponding aug-cc-pVXZ basis sets, the bond length ranges from 1.2371 to 1.2303 Å. The unpaired electron is almost exactly shared among the three O atoms in NO_3, with spin values of 0.365–0.359 $|e|$ with the cc-pVXZ basis sets, and from 0.371–0.358 $|e|$ with the aug-cc-pVXZ basis sets. The B3LYP/cc-pVDZ frequency calculation gives modes at 239.2 (e'), 801.0 (a_2''), 1140.1 (a_1'), and 1146.5 (e') cm^{-1}. At the B3LYP/aug-cc-pVDX level these modes are at 257.8 (e'), 795.6 (a_2''), 1136.0 (a_1'), and 1138.7 (e') cm^{-1}.

Figure 4 shows the B3LYP VDE and ADE as a function of increasing basis set size. As expected, convergence is slow without the diffusion functions. However, the energies are basically constant when the diffuse functions are used, reflecting the generally rapid basis set convergence of DFT methods. With the aug-cc-pV5Z basis sets the predicted VDE and ADE are 4.03 and 3.95 eV, respectively. The ADE is in excellent agreement with the experimental value of 3.92 eV. Experimentally, no difference between the ADE and VDE for NO_3^- can be distinguished, because the geometry changes are not large upon photodetachment and the 0–0 transition is the strongest peak.[39] We did similar studies of NO_3^- at the MP2 level. For NO_3^- the predicted N–O bond length ranges from 1.2625 to 1.2557 Å without the diffuse functions, and from 1.2685 to 1.2572 when the diffuse func-

TABLE II. Experimental and theoretical adiabatic (ADE) and vertical (VDE) detachment energies for $NO_3^-(H_2O)_n$ in eV.[a]

	ADE		ΔADE[b]		VDE		ΔVDE[c]	
n	Expt.	Theor.	Expt.	Theor.	Expt.	Theor.	Expt.	Theor.
0	3.92(3)	3.95			3.92(3)	4.03		
1	4.38(8)	4.56	0.46(8)	0.61	4.6 (2)	4.81	0.7(1)	0.78
2	4.88(8)	4.84	0.50(8)	0.28	5.2 (2)	5.48	0.6(1)	0.67
3	5.40(8)	4.91	0.52(8)	0.07	5.7 (2)	6.05	0.5(1)	0.57
4	5.6 (1)		0.2 (1)		5.9 (2)	6.19	0.2(1)	0.14
5	5.8 (1)		0.2 (1)		6.1 (3)	6.35	0.2(2)	0.16
6						6.53		0.18

[a]The numbers in the parentheses represent the uncertainties in the last digit. The VDE was measured from the peak maximum of the first photodetachment feature in each spectrum. The ADE was estimated by drawing a straight line at the leading edge of the first photodetachment feature and then adding a constant to the intersect with the bonding energy axis to take into account the resolution and a finite thermal effect. The reported theoretical values for $n=0-3$ were calculated at the B3LYP/aug-cc-pVTZ level. For $n=4-6$ the calculations were done at B3LYP/aug-cc-pVDZ.
[b]$\mathrm{ADE}(n)-\mathrm{ADE}(n-1)$.
[c]$\mathrm{VDE}(n)-\mathrm{VDE}(n-1)$.

Downloaded 27 Mar 2007 to 130.20.226.164. Redistribution subject to AIP license or copyright, see http://jcp.aip.org/jcp/copyright.jsp

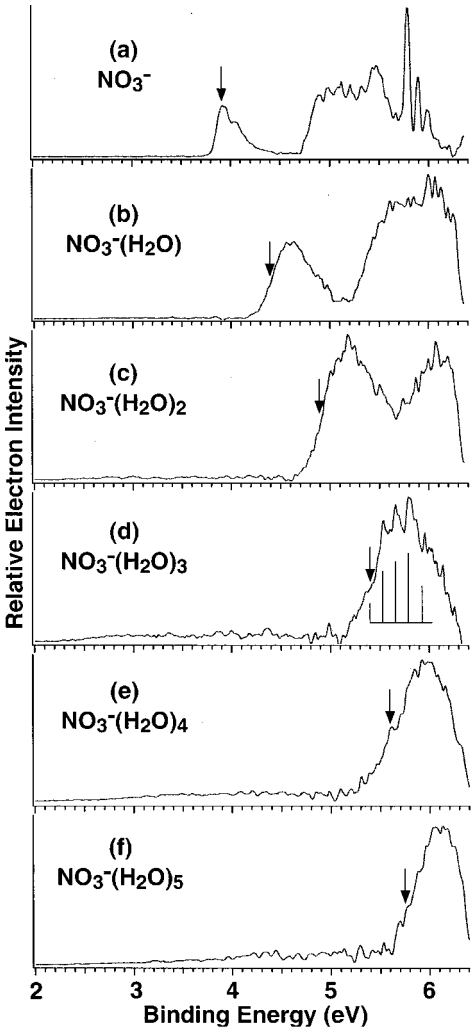

FIG. 3. Photoelectron spectra of $NO_3^-(H_2O)_n$ $(n=0-5)$ at 193 nm.

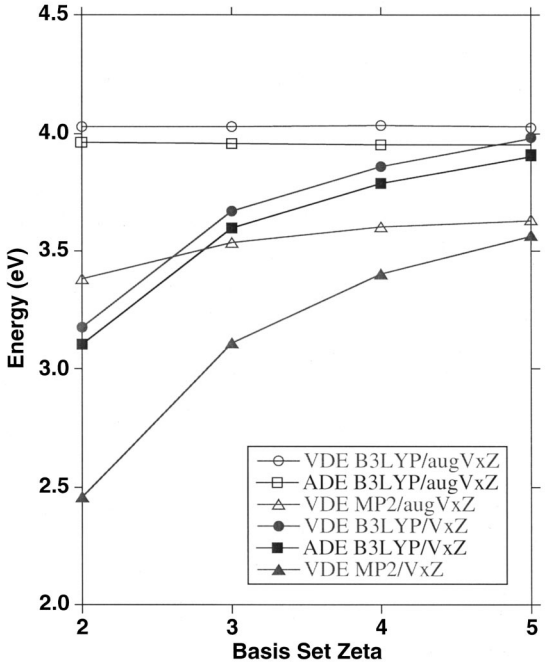

FIG. 4. Theoretical ADE and VDE for NO_3^- at the B3LYP and MP2 levels of theory as a function of basis set size.

tions are used. The MP2/cc-pVDZ frequency calculation gives modes at 727.3 (e'), 860.0 (a_2''), 1083.3 (a_1'), and 1578.3 (e') cm^{-1}. At the MP2/aug-cc-pVDZ level these are 706.6 (e'), 830.8 (a_2''), 1067.4 (a_1'), and 1487.7 (e') cm^{-1}.

Due to the problem with symmetry breaking in NO_3 at the MP2 level, we chose to only calculate the VDEs, avoiding the need for MP2 optimizations. As Fig. 4 shows, the VDE using either the cc-pVXZ or aug-cc-pVXZ basis sets appears to be converging to a value of ~3.7 eV. As expected, the diffuse functions give much more rapid convergence. Also as expected, the MP2 calculations appear to converge more slowly than the DFT calculations, particularly with the aug-cc-PVXZ basis sets. Whereas the MP2 values appear to be converging to a VDE that is too low, we investigated the effects of higher order correlation up to the CCSD(T) level. The aug-cc-pVDZ and aug-cc-pVTZ results vary widely (Table III).

From the above-mentioned data we can conclude that DFT predictions of geometries and energetics are well converged with diffuse basis sets of modest size (aug-cc-pVDZ or aug-cc-pVTZ). Thus, we used the B3LYP/aug-cc-pVTZ level for $NO_3^-(H_2O)_{1-3}$ (up to 460 basis functions) and the more computationally expedient B3LYP/aug-cc-pVDZ for $NO_3^-(H_2O)_{4-6}$ (up to 338 basis functions).

B. $NO_3^-(H_2O)$

Final optimizations of $NO_3^-(H_2O)$ were done at the B3LYP level with the aug-cc-pVTZ basis set. The lowest energy geometry has C_s symmetry [Fig. 5(a)], with one of the water hydrogens involved in a strong hydrogen bond with one NO_3^- oxygen (O . . . H distance: 1.84 Å), whereas the other water hydrogen is distant (2.50 Å). The O–H bond involved in the strong hydrogen bond is lengthened (0.98 Å) compared to the other O–H bond (0.96 Å). The ∠N–O–H angle for the strong H bond is 109.9°. Frequency calculations at the aug-cc-pVDZ and aug-cc-pVTZ levels indicate this geometry is a stable point. Constraining the geometry to C_{2v} symmetry, in which there are two equal, but apparently nonoptimal, hydrogen bonds raises the total energy by less than 0.1 kcal/mol, but this structure has one large imaginary frequency ($73i$ cm^{-1}), indicating it is not an energy minimum. Another C_s structure very close to C_{2v} is essentially isoenergetic, but also has a large imaginary frequency, and hence

TABLE III. MP2 and higher order correlation values for the VDE of NO_3^-.

	Basis set	
Correlation treatment	Aug-cc-pVDZ	Aug-cc-pVTZ
MP2	3.4	3.5
MP3	4.3	4.4
MP4(dq)	4.4	4.6
MP4(sdq)	4.2	4.3
MP4(sdtq)	3.6	3.7
CCSD	4.4	4.4
CCSD(T)	4.2	4.2

Downloaded 27 Mar 2007 to 130.20.226.164. Redistribution subject to AIP license or copyright, see http://jcp.aip.org/jcp/copyright.jsp

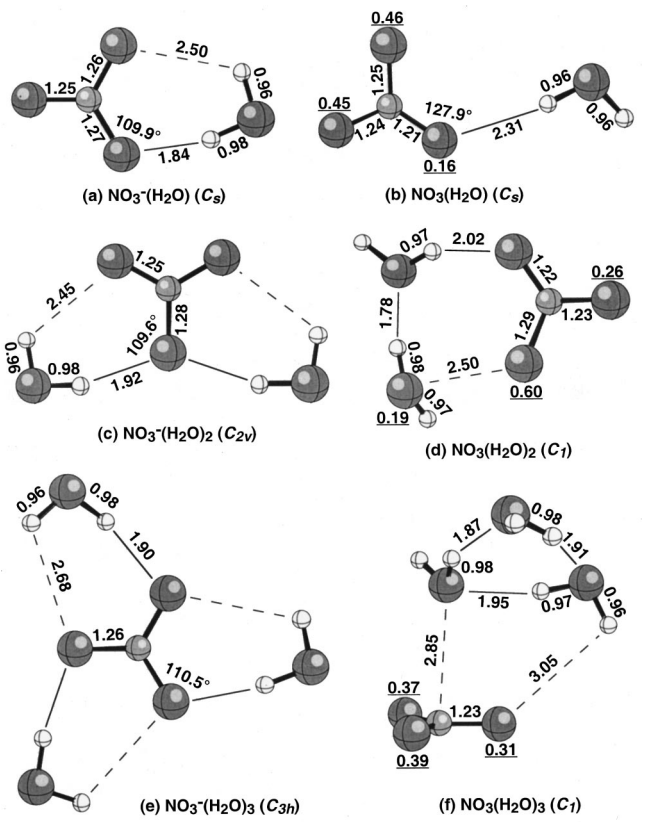

FIG. 5. B3LYP/aug-cc-pVTZ optimized geometries for (a) $NO_3^-(H_2O)$, (b) $NO_3(H_2O)$, (c) $NO_3^-(H_2O)_2$, (d) $NO_3(H_2O)_2$, (e) $NO_3^-(H_2O)_3$, and (f) $NO_3(H_2O)_3$. Selected distances in angstroms and angles in degrees. Hydrogen bonds are indicated by thin, solid lines. Electron spin values are underlined.

is not an energy minimum either. Geometry optimizations of the C_{2v} structure were also done at the MP2/aug-cc-pVDZ and MP2/aug-cc-pVTZ levels. In both cases there is one large imaginary frequency, again indicating that the C_{2v} structure is not a stable point on the potential energy surface.

The B3LYP/aug-cc-pVTZ optimized geometry of the corresponding neutral species [Fig. 5(b)] exhibits a much longer hydrogen bond (2.31 Å), implying a much weaker interaction than in the anionic complex. There is also little difference between the O–H bond lengths in the water. The ∠N–O–H angle has widened to 127.9°, as only one hydrogen on water interacts with NO_3. The unpaired electron is delocalized on the three NO_3 oxygens, with higher spin values on the two oxygens that are distant to water (~0.45 $|e|$) than that which is close (0.16 $|e|$).

C. $NO_3^-(H_2O)_2$

The optimized geometry of the $NO_3^-(H_2O)_2$ complex has C_{2v} symmetry [Fig. 5(c)], at the B3LYP level using the aug-cc-pVTZ basis set. As shown in Fig. 5(c), the two waters each form one hydrogen bond (1.92 Å) with the same oxygen of NO_3^-. The two N–O bonds pointing away from the water are shorter (1.25 Å) than the N–O bond involved in the hydrogen bonds to waters (1.28 Å). Similarly, the water O–H bond involved in the strong hydrogen bond is longer (0.98 Å) than the other OH (0.96 Å) that is more distant from NO_3^-.

The optimized geometry for the neutral complex is much different [Fig. 5(d)]. The two waters are both on one of the edges of NO_3, with one of the water hydrogens interacting with NO_3 oxygen at a distance of 2.02 Å. The three N–O bond lengths in NO_3 are similar, with values of 1.22, 1.23, and 1.29 Å. The two waters form a distorted dimer structure, with a hydrogen bond distance of 1.78 Å, notably shorter than the distance predicted for the isolated water dimer (1.95 Å, see the following). This geometry implies that the interaction between NO_3 and water is no longer competitive relative to the intrawater hydrogen bonding. The unpaired electron is delocalized on two of the three NO_3 oxygens (0.60 and 0.26 $|e|$) and an appreciable spin on one of the water oxygens (0.19 $|e|$).

D. $NO_3^-(H_2O)_3$

The optimized geometry of $NO_3^-(H_2O)_3$ at the B3LYP/aug-cc-pVTZ level has C_{3h} symmetry [Fig. 5(e)]. Each water forms one hydrogen bond with an oxygen of NO_3 (O . . . H distance: 1.90 Å). The ∠N–O–H angle is 110.5°, consistent with the hydrogen interacting with a lone pair on oxygen. The water O–H involved in the strong H bond is longer (0.98 Å) than the other OH bond (0.96 Å), which is 2.68 Å from the NO_3^- oxygen. The N–O bond lengths are 1.26 Å. A frequency calculation at the 3BLYP/aug-cc-pVDZ level gives a value of 1079 cm^{-1} for a mode that is primarily N–O symmetric stretch, with very small contributions from the three H_2O.

The B3LYP/aug-cc-pVTZ optimized geometry of the neutral complex [Fig. 5(f)] again indicates that water–water interactions are dominating the water–NO_3 interactions, similar to that found in $NO_3(H_2O)_2$ [Fig. 5(d)]. The closest interactions between NO_3 and water are a N . . . O distance of 2.85 Å and a very weak hydrogen bond of 3.05 Å [Fig. 5(f)]. In contrast, the water–water hydrogen bond lengths (1.87–1.95 Å) are similar or shorter compared to those predicted for the isolated water dimer (1.95 Å, see the following). The unpaired electron is delocalized on the three NO_3 oxygens, with values of 0.31–0.39 $|e|$. The fact that the neutral complexes optimize to geometries much different than those of the anions makes the interpretation of the theoretical ADEs problematic (see the following). Thus, we did not theoretically examine the geometries of the larger neutral complexes.

E. $NO_3^-(H_2O)_4$

The three H_2O in $NO_3^-(H_2O)_3$ appears to form an inner solvation shell around NO_3^-. Thus, in the optimized geometry of $NO_3^-(H_2O)_4$ at B3LYP/aug-cc-pVDZ level, the fourth water H bonds to one of the inner sphere waters, without direct interaction with NO_3^- [Fig. 6(a)]. Most of the C_{3h} geometry of the $NO_3^-(H_2O)_3$ complex is preserved, although small changes in distances and angles distort the structure from true C_{3h} symmetry. The three N–O bond lengths are 1.256, 1.260, and 1.264 Å. The hydrogen bond lengths are

Downloaded 27 Mar 2007 to 130.20.226.164. Redistribution subject to AIP license or copyright, see http://jcp.aip.org/jcp/copyright.jsp

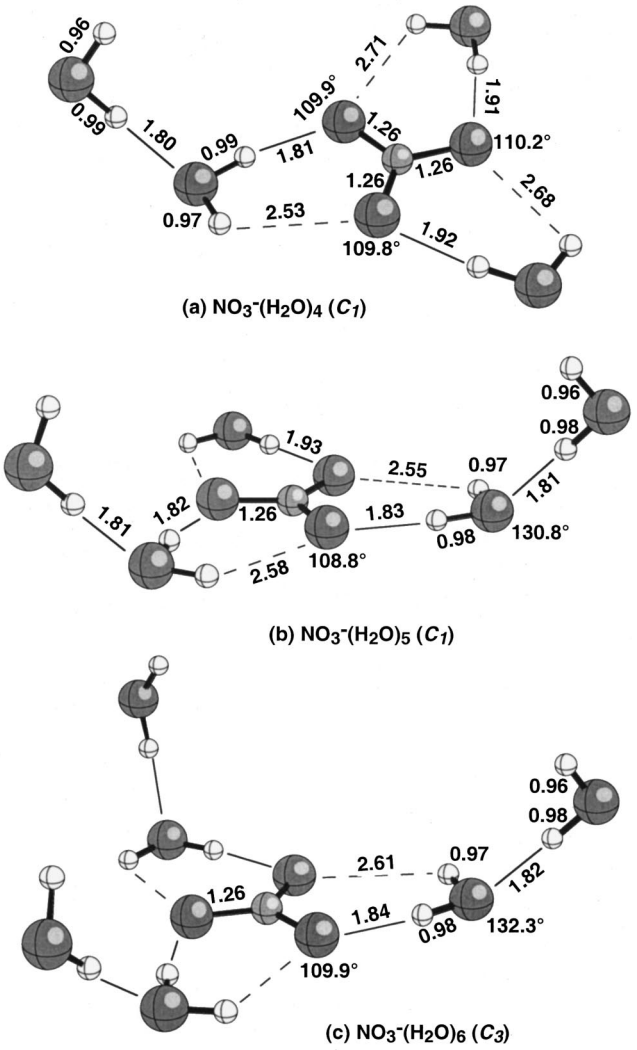

FIG. 6. B3LYP/aug-cc-pVDZ optimized geometries for (a) $NO_3^-(H_2O)_4$, (b) $NO_3^-(H_2O)_5$, and (c) $NO_3^-(H_2O)_6$. Selected distances in angstroms and angles in degrees. Hydrogen bonds are indicated by thin, solid lines.

1.91 and 1.92 Å for the two inner sphere waters not involved with the second shell water, whereas the distance is 1.81 Å for the other water. The hydrogen bond lengths between the first and second solvation shell waters are 1.80 Å. The ∠N–O–H angles are 109.0°–110.2°. The angles between the coordinating hydrogen of the second solvation shell water and the plane of the first shell water is 128.7°. The asymmetry in the two O–H bond lengths of each water is consistent with the H-bonding network, with those O–H bonds involved in strong H bonding being ~0.02 Å longer.

F. $NO_3^-(H_2O)_5$

In $NO_3^-(H_2O)_5$ optimized at the B3LYP/aug-cc-pVDZ level [Fig. 6(b)], the additional H_2O again adds to the second solvation shell, forming a hydrogen bond with one of the inner sphere oxygens. As was the case with $NO_3^-(H_2O)_4$, the C_{3h} geometry of the inner sphere solvation shell remains relatively unperturbed. The three bond distances between the inner sphere water hydrogens and NO_3^- oxygens are 1.82, 1.83, and 1.93 Å, with the two shorter distances associated with the second coordination shell. The ∠N–O–H angles range from 108.8° to 110.2°, similar to the angles seen in the smaller clusters. The hydrogen bonds between the first and second solvation shell waters are 1.81 Å. The angles between the corresponding hydrogen of the second solvation shell water and the plane of the first shell water is 130.8°. There is again a ~0.02 Å asymmetry in the two O–H bond lengths in each H_2O due to the hydrogen bonding interactions.

G. $NO_3^-(H_2O)_6$

The $NO_3^-(H_2O)_6$ cluster optimized at the B3LYP/aug-cc-pVDZ level [Fig. 6(c)] has three waters in both the first and second solvation shells with C_3 symmetry. The N–O bond lengths are 1.26 Å, the inner sphere hydrogen bond lengths are 1.84 Å, and the hydrogen bond lengths between the first and second solvation shell waters are 1.82 Å. The ∠N–O–H angles are 109.9°. There is a slight deviation from planarity in the central $NO_3^-(H_2O)_3$ part of the cluster, which lowers its local symmetry from C_{3h} to C_3. The angles between the coordinating hydrogens of the second solvation shell waters and the plane of the first shell waters are 132.3°. The asymmetry in the two O–H bond lengths of each water is consistent with the H-bonding network, with those O–H bonds involved in the strong H bonding being ~0.02 Å longer.

H. Microsolvation and the water dimer

The waters of the second solvation shell bind to the inner sphere waters in a geometry similar to that in the water dimer. To characterize the geometry in more detail, we also optimized $(H_2O)_2$. In the B3LYP/aug-cc-pVDZ optimized $(H_2O)_2$, the hydrogen bond length is 1.95 Å. This compares to values of 1.81–1.82 Å in the $NO_3^-(H_2O)_n$ clusters involving four to six waters. The angle between the plane of the acceptor water and the H bond is 125.3° in $(H_2O)_2$, whereas it is 128.7°–132.3° in the $NO_3^-(H_2O)_n$ clusters. The H-bond energy in $(H_2O)_2$ is −4.7 kcal/mol at this level of theory. Little is changed at the B3LYP/aug-cc-pVDZ level; the hydrogen bond length is 1.95 Å and the H-bond energy is −4.6 kcal/mol.

I. Hydration energies

The energy of interaction between each successive water and NO_3^- was determined at the B3LYP/aug-cc-pVDZ level of theory. The first water binds to NO_3^- with an energy of −14.8 kcal/mol. As each additional water is added, the incremental hydration energy becomes smaller, being −12.7, −11.4, −10.1, −9.7, and −9.3 kcal/mol for two to six waters, respectively. This is consistent with waters 4–6 not directly interacting with NO_3^-. The limited calculations at the B3LYP/aug-cc-pVTZ level for one to three waters give values of −14.5, −12.4, and −11.1 kcal/mol, respectively, very close to those at the lower level of theory. These results suggest that the basis set superposition error is not large at the B3LYP/aug-cc-pVDZ level of theory. The binding energies for the water in the second solvation shell are still approximately twice as large as the hydrogen bonding energy

Downloaded 27 Mar 2007 to 130.20.226.164. Redistribution subject to AIP license or copyright, see http://jcp.aip.org/jcp/copyright.jsp

we calculated for the neutral water dimer, indicating the many-body effects and the long-range influence of the negative charge.

As noted previously, the optimized geometries of the clusters indicate very weak interactions between the neutral NO_3 and water. Indeed the B3LYP/aug-cc-pVDZ binding energy for $NO_3(H_2O)$ is only 0.8 kcal/mol. For $NO_3(H_2O)_2$, the incremental binding energies increases (6.9 kcal/mol), reflecting the larger relative strength of the water–water H bond. This binding energy is lower than that of the anionic cluster, but greater than that of the isolated water dimer. The incremental binding energy of the third water is 9.6 kcal/mol, consistent with its ability to form two hydrogen bonds to other waters.

J. VDEs and ADEs

The theoretical ADEs and VDEs are compared with the experimental values in Table II. As expected, the ADEs, and VDEs increase as waters are added. The predicted VDEs at the B3LYP/aug-cc-pVXZ levels of theory range from 4.03 to 6.53 eV for $n=0-6$. The incremental increase in electron binding energy is larger for clusters with n up to 3 waters, whereas it is smaller for the waters that form the second solvation shell. The ADEs were only calculated for $n=0-3$. These values range from 3.95 to 4.91 eV.

VI. DISCUSSION

A. NO_3^-/NO_3

The three states observed in our spectra ($X\ ^2A_2'$, $A\ ^2E''$, $B\ ^2E'$) in Fig. 1 result from detaching one electron from the corresponding valence orbitals, $1a_2'$, $1e''$, and $3e'$ of NO_3^-, respectively. These are all essentially O $2p$ lone pairs, the $1a_2'$ and $3e'$ orbitals being in the molecular plane and $1e''$ perpendicular to the plane.[37,38] Our results for the X and A bands at the lower resolution are consistent with the previous higher resolution study by Neumark *et al.*, who analyzed these two bands in detail.[39] Our discussion will only focus on the B band, which was not observed before. The apparent slight intensity changes in the vibrational progressions in the X and A bands compared to the previous spectrum were due to the lower resolution in the current spectra, resulting in overlapping features. Our DFT results (Fig. 4) are in good agreement with the experimental data. The theoretical and experimental VDEs differ by only ~0.1 eV, whereas the ADEs are essentially identical. The limited MP2 results agree less well with the experimental data: the predicted VDE is too low by ~0.3 eV (Fig. 4). The predicted values (257.8 and 1136 cm^{-1}) for the two observed frequencies for the ground state of NO_3 are also in reasonable agreement with the experimental values of 320 and 1050 cm^{-1} (Table I).

In contrast to the X and A bands, the B band exhibited only one vibrational progression with an 850 cm^{-1} frequency [Fig. 1(b)]. This simple progression indicates that there is only one totally symmetric mode active in the detachment transition from the ground state of NO_3^- to the $B\ ^2E'$ state of NO_3. The excitation energy observed in our PES spectrum (1.86 eV) is in excellent agreement with previous optical experiments (Table I). Of the three frequencies (930, 1450, and 850 cm^{-1}) observed in the absorption spectra,[47] the 930 cm^{-1} frequency was assigned to the symmetric stretch, whereas the 1450 cm^{-1} frequency might be due to the antisymmetric stretch. Nelson *et al.* assigned the 820 cm^{-1} frequency in their absorption spectrum to the in-plane symmetric bending mode with a C_{2v} structure for the $B\ ^2E'$ state.[32]

For D_{3h} NO_3, there are four normal modes: symmetric stretching (ν_1, a_1), out-of-plane bending (ν_2, a_2''), antisymmetric stretching (ν_3, e'), and in-plane bending (ν_4, e'). The symmetric stretching mode (ν_1) is the only totally symmetric mode. The average frequency of ν_1 of the $B\ ^2E'$ state determined previously is 930 cm^{-1}, larger than the 850 cm^{-1} frequency observed in our spectrum. However, under C_{2v} symmetry, the two degenerate normal modes will split, resulting in six nondegenerate modes: $(\nu_1, a_1') \rightarrow (\nu_1, a_1)$; $(\nu_2, a_2'') \rightarrow (\nu_4, b_1)$; $(\nu_3, e') \rightarrow (\nu_2, a_1) + (\nu_5, b_2)$; and $(\nu_4, e') \rightarrow (\nu_3, a_1) + (\nu_6, b_2)$, now with three totally symmetric modes.[30] We assigned the observed vibrational progression to the in-plane ν_3 bending mode under C_{2v}. This assignment, consistent with the literature,[32] implies that the geometry of the $B\ ^2E'$ state of NO_3 has C_{2v} symmetry, with the N–O bond length being almost the same as that of NO_3^- since there is little Franck–Condon factor in the symmetric N–O stretching mode in the PES spectrum. The reduced symmetry in the B state of NO_3 is also consistent with the Jahn–Teller effect, expected to be operative in the degenerate $B\ ^2E'$ state. The only appreciable change between the D_{3h} NO_3^- and the B state of the C_{2v} NO_3 is the O–N–O bond angles. This assignment is consistent with the nature of the $3e'$ orbital (involving in-plane O–O interaction),[37,38] from which an electron is detached.

B. Comparison with previous calculations on $NO_3^-(H_2O)_n$

There are three previous calculations on the ground state structures and energies of small nitrate water clusters $NO_3^-(H_2O)_n$ by Kelley *et al.* ($n=1,2$),[10] Schaefer *et al.* ($n=1$),[26] and Synder *et al.* ($n=1-3$).[27] All the previous calculations conclude that the first water strongly interacts with NO_3^-, forming two strong hydrogen bonds with a C_{2v} structure. Our calculation also indicates two hydrogen bonds between the first water and NO_3^-, but the two hydrogen bonds are asymmetric, giving C_s symmetry. The C_{2v} geometry is a minimum at the Hartree–Fock level, but our frequency calculations indicate it is not a minimum when correlation is included, either by DFT or MP2 methods. The second water was predicted by Kelly *et al.*[10] to interact with NO_3^- via a single hydrogen bond, different from the result by Snyder *et al.*,[27] who proposed that the second water still preferred to be doubly hydrogen bond to NO_3^-. Our calculation predicts that the second water also forms two asymmetric hydrogen bonds to NO_3^- [Fig. 5(c)].

The only previous calculation on $NO_3^-(H_2O)_3$ was by Snyder *et al.*,[27] who found a D_{3h} structure with each H_2O forming two equal hydrogen bonds to NO_3^-. A similar structure was predicted for the $PO_3^-(H_2O)_3$ cluster by Wu and Houk.[48] In contrast, our calculation predicts $NO_3^-(H_2O)_3$ to

Downloaded 27 Mar 2007 to 130.20.226.164. Redistribution subject to AIP license or copyright, see http://jcp.aip.org/jcp/copyright.jsp

be planar, but with C_{3h} symmetry, in which each water forms a strong and weak hydrogen bond to NO_3^- [Fig. 5(e)]. We again attribute this difference to the effects of electron correlation, which was not included in the earlier calculations.

C. The first solvation shell of NO_3^-:$NO_3^-(H_2O)_3$

The fact that only the PES spectrum of $NO_3^-(H_2O)_3$ was vibrationally resolved [Fig. 3(d)] suggests that this complex has higher symmetry than the other solvated species, consistent with our theoretical prediction of the C_{3h} geometry for $NO_3^-(H_2O)_3$. Similarly, our unscaled theoretical frequency for the symmetric stretch in this system is 1079 cm^{-1}, in good agreement with the experimental value of 1000 cm^{-1}. The theoretical and experimental symmetric stretching frequency also agrees very well with the bulk solution value of 1050 cm^{-1}.[9,10]

The incremental increase in VDEs ranges from 0.7 to 0.5 eV for the first three waters, but reduced to 0.20 eV for $n=4$ and 5 (Table II), indicating that the first three water molecules interact with the nitrate core much more strongly than the fourth and fifth waters. This result again agrees with the theoretically optimized geometries, which predict that the first three H_2O molecules bind directly to NO_3^-, whereas the next three H_2O form the second solvation shell.

The sequential hydration energies for $NO_3^-(H_2O)_n$ are also consistent with three H_2O forming the first solvation shell. There have been several previous experimental measurements of the solvation enthalpy and free energy of NO_3^-. For the addition of the first through third waters, our theoretical results (B3LYP/aug-cc-pVDZ frequencies scaled by 0.95) predict binding enthalpies of -13.3, -11.2, and -9.9 kcal/mol. These values compare reasonably to experimental values of -14.6, -14.3, and -13.8 from Castleman *et al.*[25] and -12.4 kcal/mol (for the first water) from Kebarle *et al.*[24] The predicted free energies of solvation for the first through third waters are -6.1, -2.9, and -2.5 kcal/mol at 298.15 K. Comparable experimental values are -7.1, -5.2, and -3.9 kcal/mol.[24,25] As was the case for the enthalpies, the predicted value for the addition of the first water is in better agreement than the values for the second and third. Whereas the theoretical estimates are strongly effected by the low frequencies, which are difficult to predict in relatively weakly bound systems such as these, we only expect qualitative agreement.

D. Comparison of theoretical with experimental ADEs

The substantial difference in geometry between the anionic and neutral complexes (Fig. 5) hampers the interpretation of the theoretical ADEs. Electron detachment is a vertical process; the final and initial states have the same geometries during the electron detachment. When the equilibrium geometries of the anion and the neutral are similar, there is a significant Franck–Condon factor for the 0–0 transition. In this case, we can experimentally determine a true ADE with reasonable accuracy. However, as the theoretical results demonstrate, the neutral complexes, particularly $NO_3(H_2O)_2$ and $NO_3(H_2O)_3$, optimize to geometries that are much different from those of the anionic complexes. Apparently, in these cases, the true ADEs cannot be measured experimentally and the numbers given in Table I should be viewed as upper limits. The apparent excellent agreement between the experimental and theoretical ADE for $NO_3^-(H_2O)_2$ might be fortuitous. Since our focus for the solvated species is on the anions, the VDEs in general provide a much better comparison between the experiment and theory. Nevertheless, the experimental ADEs showed exactly the same trend as the VDEs.

VII. CONCLUSIONS

We report a theoretical and photoelectron spectroscopic study of $NO_3^-(H_2O)_n$ $(n=0-6)$. The current PES spectra of bare NO_3^- at high photon energies revealed a simple vibrational progression of the second excited state ($B\ ^2E'$) of NO_3. The observed 850 cm^{-1} frequency was assigned to the in-plane symmetric bending mode of a C_{2v} NO_3. The electron binding energies of the solvated clusters $NO_3^-(H_2O)_n$ were found to increase with n. The incremental increase of the vertical electron binding energies ranges from 0.7 to 0.5 eV for the first three waters and drops to 0.20 eV for $n=4$ and 5. Broad and diffuse spectra were observed for the solvated species, except for $NO_3^-(H_2O)_3$, for which a partially vibrationally resolved spectrum was obtained at 193 nm. Our theoretical predictions of the vertical electron binding energies agree well with the experimental results. The predicted geometries indicate the first three waters form the first solvation shell around NO_3^-, giving rise to a high symmetry C_{3h} $NO_3^-(H_2O)_3$. The C_{3h} $NO_3^-(H_2O)_3$ appears to be a rather robust solvation structure since it is largely preserved as the fourth to sixth water were added to the second solvation shell. Our observed N–O stretching frequency in the C_{3h} $NO_3^-(H_2O)_3$ is already very close to that in bulk nitrate. Thus the current result suggests that in bulk aqueous nitrate solution the first solvation shell of NO_3^- may also involve only three water molecules.

ACKNOWLEDGMENTS

This work was supported by the U.S. Department of Energy, Office of Basic Energy Sciences, Chemical Science Division and partially by The Petroleum Research Fund, administered by the American Chemical Society. The work was performed at the W. R. Wiley Environmental Molecular Sciences Laboratory, a national scientific user facility sponsored by DOE's Office of Biological and Environmental Research and located at Pacific Northwest National Laboratory, which is operated for DOE by Battelle.

[1] H. Ohtaki and T. Radnai, Chem. Rev. **93**, 1157 (1993).
[2] S. S. Xantheas, J. Phys. Chem. **100**, 9703 (1996).
[3] O. M. Cabarcos, C. J. Weinheimer, J. M. Lisy, and S. S. Xantheas, J. Chem. Phys. **110**, 5 (1999).
[4] G. Markovich, S. Pollack, R. Giniger, and O. Cheshnovsky, J. Chem. Phys. **101**, 9344 (1994).
[5] P. Ayotte, G. H. Weddle, and M. A. Johnson, J. Chem. Phys. **110**, 7129 (1999).
[6] J. H. Choi, K. T. Kuwata, Y. B. Cao, and M. Okumura, J. Phys. Chem. A **102**, 503 (1998).
[7] L. Lehr, M. T. Zanni, C. Frischkorn, R. Weinkauf, and D. M. Neumark, Science **284**, 635 (1999).

Downloaded 27 Mar 2007 to 130.20.226.164. Redistribution subject to AIP license or copyright, see http://jcp.aip.org/jcp/copyright.jsp

[8] B. J. Greenblatt, M. T. Zanni, and D. M. Neumark, Science **276**, 1675 (1997).
[9] J. M. Weber, J. A. Kelley, S. B. Nielsen, P. Ayotte, and M. A. Johnson, Science **287**, 2461 (2000).
[10] J. M. Weber, J. A. Kelley, W. H. Robertson, and M. A. Johnson, J. Chem. Phys. **114**, 2698 (2001).
[11] X. B. Wang, J. B. Nicholas, and L. S. Wang, J. Chem. Phys. **113**, 10837 (2000).
[12] P. A. Bergstrom, J. Lindgren, and O. Kristiansson, J. Phys. Chem. **95**, 8575 (1991).
[13] M. Nakahara and K. Emi, J. Chem. Phys. **99**, 5418 (1993).
[14] Y. Ikushima, N. Saito, and M. Arai, J. Phys. Chem. B **102**, 3029 (1998).
[15] M. R. Waterland and A. M. Kelley, J. Chem. Phys. **113**, 6760 (2000).
[16] M. R. Waterland, D. Stockwell, and A. M. Kelley, J. Chem. Phys. **114**, 6249 (2001).
[17] R. S. Narcisi, A. D. Bailey, L. D. Lucca, C. Sherman, and D. M. Thomas, J. Atmos. Terr. Phys. **33**, 1147 (1971).
[18] R. Arnold, J. Kissel, D. Krankowsky, H. Weider, and J. Zahringer, J. Atmos. Terr. Phys. **33**, 1169 (1971).
[19] P. M. Aker, J. X. Zhang, and W. Nichols, J. Chem. Phys. **110**, 2202 (1999).
[20] F. C. Fehsenfeld and E. E. Ferguson, J. Chem. Phys. **61**, 3181 (1974).
[21] J. V. Seeley, T. M. Miller, and A. A. Viggiano, J. Chem. Phys. **105**, 2127 (1996).
[22] S. Parthiban and T. J. Lee, J. Chem. Phys. **109**, 525 (1998).
[23] J. D. Payzant, R. Yamadagni, and P. Kebarle, Can. J. Chem. **49**, 3308 (1971).
[24] A. T. Blades, J. S. Klassen, and P. Kebarle, J. Am. Chem. Soc. **117**, 10563 (1995).
[25] N. Lee, R. G. Keesee, and A. W. Castleman, Jr., J. Chem. Phys. **72**, 1089 (1980).
[26] M. Shen, Y. Xie, H. F. Schaefer III, and C. A. Deakyne, J. Chem. Phys. **93**, 3379 (1990).
[27] J. M. Howell, A. M. Sapse, E. Singman, and G. Snyder, J. Phys. Chem. **86**, 2345 (1982).
[28] M. Hotokka and P. Pyykkö, Chem. Phys. Lett. **157**, 415 (1989).
[29] J. H. Seinfeld, Science **243**, 745 (1989).
[30] B. Kim, P. L. Hunter, and H. S. Johnston, J. Chem. Phys. **96**, 4057 (1992).
[31] T. Ishiawata, I. Fujiwara, Y. Naruge, K. Obi, and I. Tanaka, J. Phys. Chem. **87**, 1349 (1983).
[32] H. H. Nelson, L. Pasternack, and J. R. McDonald, J. Chem. Phys. **79**, 4279 (1983); J. Phys. Chem. **87**, 1286 (1983).
[33] W. J. Marinelli, D. M. Swanson, and H. S. Johnston, J. Chem. Phys. **76**, 2864 (1982).
[34] R. A. Graham and H. S. Johnston, J. Phys. Chem. **82**, 254 (1978).
[35] E. Hirota, T. Ishiwata, K. Kawaguchi, M. Fujitake, N. Ohashi, and I. Tanaka, J. Chem. Phys. **107**, 2829 (1997).
[36] D. Heryadi and D. L. Yeager, J. Chem. Phys. **112**, 4572 (2000).
[37] M. Mayer, L. S. Cederbaum, and H. Köppel, J. Chem. Phys. **100**, 899 (1994).
[38] W. Eisfeld and K. Morokuma, J. Chem. Phys. **113**, 5587 (2000); **114**, 9430 (2001), and references therein.
[39] A. Weaver, D. W. Arnold, S. E. Bradforth, and D. M. Neumark, J. Chem. Phys. **94**, 1740 (1991).
[40] L. S. Wang, C. F. Ding, X. B. Wang, and S. E. Barlow, Rev. Sci. Instrum. **70**, 1957 (1999).
[41] A. D. Becke, J. Chem. Phys. **98**, 5648 (1993).
[42] T. H. Dunning, Jr., J. Chem. Phys. **90**, 1007 (1989).
[43] R. A. Kendall, T. H. Dunning, Jr., and R. A. Harrison, J. Chem. Phys. **96**, 6796 (1992).
[44] C. Møller and M. S. Plesset, Phys. Rev. **46**, 618 (1934).
[45] J. A. Pople, M. Head-Gordon, K. Raghavachari, and G. W. Trucks, Chem. Phys. Lett. **164**, 185 (1989).
[46] M. J. Frisch, G. W. Trucks, H. B. Schlegel *et al.*, GAUSSIAN 98, Revision A, Gaussian, Inc., Pittsburgh, PA, 1998.
[47] M. E. Jacox, J. Phys. Chem. Ref. Data Monogr. **3**, 207 (1994).
[48] Y. D. Wu and K. N. Houk, J. Am. Chem. Soc. **115**, 11997 (1993).

Downloaded 27 Mar 2007 to 130.20.226.164. Redistribution subject to AIP license or copyright, see http://jcp.aip.org/jcp/copyright.jsp